

Bidirectional Loss Function for Label Enhancement and Distribution Learning[★]

Xinyuan Liu^a, Jihua Zhu^{a,*}, Qinghai Zheng^a, Zhongyu Li^a, Ruixin Liu^a and Jun Wang^b

^aLab of VCAML, School of Software Engineering, Xi'an Jiaotong University, Xi'an 710049, People's Republic of China

^bSchool of Communication and Information Engineering, Shanghai University, Shanghai 200072, People's Republic of China

ARTICLE INFO

Keywords:

Label Distribution Learning

Label Enhancement

Bi-directional Loss

ABSTRACT

Label distribution learning (LDL) is an interpretable and general learning paradigm that has been applied in many real-world applications. In contrast to the simple logical vector in single-label learning (SLL) and multi-label learning (MLL), LDL assigns labels with a description degree to each instance. In practice, two challenges exist in LDL, namely, how to address the dimensional gap problem during the learning process of LDL and how to exactly recover label distributions from existing logical labels, i.e., Label Enhancement (LE). For most existing LDL and LE algorithms, the fact that the dimension of the input matrix is much higher than that of the output one is always ignored and it typically leads to the dimensional reduction owing to the unidirectional projection. The valuable information hidden in the feature space is lost during the mapping process. To this end, this study considers bidirectional projections function which can be applied in LE and LDL problems simultaneously. More specifically, this novel loss function not only considers the mapping errors generated from the projection of the input space into the output one but also accounts for the reconstruction errors generated from the projection of the output space back to the input one. This loss function aims to potentially reconstruct the input data from the output data. Therefore, it is expected to obtain more accurate results. Finally, experiments on several real-world datasets are carried out to demonstrate the superiority of the proposed method for both LE and LDL.

1. Introduction

Learning with ambiguity has become one of the most prevalent research topics. The traditional way to solve machine learning problems is based on single-label learning (SLL) and multi-label learning (MLL) Tsoumakas and Katakis (2007); Xu, Yang, Yu, Yu, Yang and Tsang (2016). Concerning the SLL framework, an instance is always assigned to one single label, whereas in MLL an instance may be associated with several labels. The existing learning paradigms of SLL and MLL are mostly based on the so-called *problem transformation*. However, neither SLL nor MLL address the problem stated as “at which degree can a label describe its corresponding instance,” i.e., the labels have different importance on the description of the instance. It is more appropriate for the importance among candidate labels to be different rather than exactly equal. Taking the above problem into account, a novel learning paradigm called label distribution learning (LDL) Geng and Ji (2013) is proposed. Compared with SLL and MLL, LDL labels an instance with a real-valued vector that consists of the description degree of every possible label to the current instance. Detail comparison is visualized in Fig. 1. Actually, LDL can be regarded as a more comprehensive form of MLL and SLL. However, the tagged training sets required by LDL are extremely scarce owing to the heavy burden of manual annotation. Considering the fact that it is difficult to directly attain the annotated label distribution, a process called label enhancement (LE) Xu, Tao and Geng (2018) is also proposed to recover the label distributions from logical labels. Taking LE algorithm, the logical label $l \in \{0, 1\}^c$ of conventional MLL dataset can be recovered into the label distribution vector by mining the topological information of input space and label correlation He, Yang, Gao, Liu and Yin (2019).

Many relevant algorithms of LDL and LE have been proposed in recent years. These algorithms have progressively boosted the performance of specific tasks. For instance, LDL is widely applied in facial age estimation application. Geng et al. Geng, Wang and Xia (2014) proposed a specialized LDL framework that combines the maximum entropy model Berger, Pietra and Pietra (1996) with IIS optimization, namely IIS-LDL. This approach not only achieves better

[★]This work is supported by the National Natural Science Foundation of China under Grant No. 61573273.

*Corresponding author, email: zhujh@xjtu.edu.cn.

ORCID(s): 0000-0002-3081-8781 (J. Zhu)

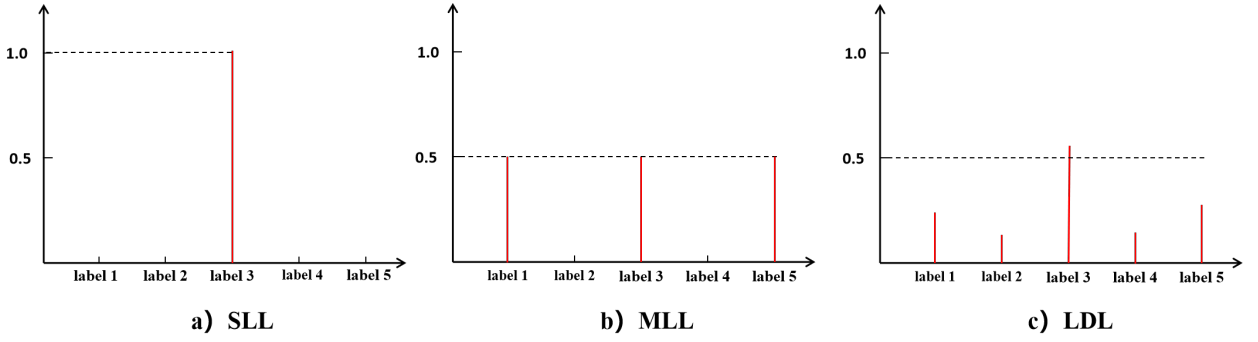


Figure 1: Visualized comparison among SLL, MLL and LDL

performance than other traditional machine learning algorithms but also becomes the foundation of the LDL framework. In other works, Yang et al. & Fan, Liu, Li, Guo, Samal, Wan and Li (2017) attempt to take into account both facial geometric and convolutional features resulted in remarkably improving efficiency and accuracy. As mentioned above, the difficulty of acquiring labeled datasets restricts the development of LDL algorithms. After presenting several LE algorithms, Xu et al. Xu, Lv and Geng (2019b) adapted LDL into partial label learning (PLL) with recovered label distributions via LE. Although these methods have achieved significant performance, one potential problem yet to be solved is that they suffer from the discriminative information loss problem, which is caused by the dimensional gap between the input data matrix and the output one. Importantly, it is entirely possible that these existing methods miss the essential information that should be inherited from the original input space, thereby degrading the performance.

As discussed above, the critical point of previous works on LDL and LE is to establish a suitable loss function to fit label distribution data. In previous works, only a unidirectional projection $\mathcal{X} \mapsto \mathcal{Y}$ between input and output space is learned. In this paper, we present a bi-directional loss function with a comprehensive reconstruction constraint. Such function can be applied in both LDL and LE to maintain the latent information. Inspired by the auto-encoder paradigm Kodirov and Gong (2017); Cheng, Zhao, Wang and Pei (2019), our proposed method builds the reconstruction projection $\mathcal{Y} \mapsto \mathcal{X}$ with the mapping projection to preserve the otherwise lost information. More precisely, optimizing the original loss is the *mapping* step, while minimizing the *reconstruction* error is the reconstruction step. In contrast to previous loss functions, the proposed loss function aims to potentially reconstruct the input data from the output data. Therefore, it is expected to obtain more accurate results than other related loss functions for both LE and LDL problems. Adequate experiments on several well-known datasets demonstrate that the proposed loss function achieves superior performance.

The main contributions of this work are delivered as:

- 1) the reconstruction projection from label space to instance space is considered for the first time in the LDL and LE paradigms;
- 2) a bi-directional loss function that combines mapping error and reconstruction error is proposed;
- 3) the proposed method can be used not only in LDL but also for LE.

We organize the rest of this paper as follows. Firstly, related work about LDL and LE methods is reviewed in Section 2. Secondly, the formulation of LE as well LDL and the proposed methods, i.e., BD-LE and BD-LDL are introduced in Section 3. After that, the results of comparison experiment and ablation one are shown in Section 4. The influence of parameters is also discussed in Section 4. Finally, conclusions and future work exploration are summarized in section 5.

2. Related work

In this section, we briefly summarize the related work about LDL and LE methods.

2.1. Label Distribution Learning

The proposed LDL methods mainly focus on three aspects, namely model assumption, loss function, and the optimization algorithm. The maximum entropy model Berger et al. (1996) is widely used to represent the label distribution

in the LDL paradigm Xu, Shang and Shen (2019c); Ren, Jia, Li and Zhao (2019b). Maximum entropy model naturally agrees with the character of description degree in LDL model. However, such an exponential model is sometimes not comprehensive enough to accomplish a complex distribution. To overcome this issue, Gent et al. Xing, Geng and Xue (2016) proposed a LDL family based on a boosting algorithm to extend the traditional LDL model. Inspired by the M-SVR algorithm, LDVSR Geng and Hou (2015) is designed for the movie opinion prediction task. Furthermore, CPNN Geng, Yin and Zhou (2013) combines a neural network with the LDL paradigm to improve the effectiveness of facial age estimation applications. What's more, recent work Ren, Jia, Li, Chen and Li (2019a); Xu and Zhou (2017) has proved that linear model is also able to achieve a relatively strong representation ability and a satisfying result. As reviewed above, most existing methods build the mapping from feature space to label space in an unidirectional way so that it is appropriate to take the bi-directional constraint into consideration.

Concerning the loss function, LDL aims at learning the model to predict unseen instances's distributions which are similar to the true ones. The criteria to measure the distance between two distributions, such as the Kullback-Leibler (K-L) divergence, is always chosen as the loss function Jia, Li, Liu and Zhang (2018); Geng, Smith-Miles and Zhou (2010). Owing to the asymmetry of the K-L divergence, Jeffery's divergence is used in xxx Zhou, Xue and Geng (2015) to build LDL model for facial emotion recognition. For the sake of easier computation, it is reasonable to adopt the Euclidean distance in a variety of tasks, e.g., facial emotion recognition Jia, Zheng, Li, Zhang and Li (2019b).

Regarding the optimization method, SA-IIS Geng (2016) utilizes the improved iterative scaling (IIS) method whose performance is always worse Malouf (2002) than the other optimization. Fortunately, by leveraging the L-BFGS Nocedal and Wright (2006) optimization method, we maintain the balance between efficiency and accuracy, especially in SA-BFGS Geng (2016) and EDL Zhou et al. (2015). With the complexity of proposed model greater, the number of parameters to be optimized is more than one. Therefore, it is more appropriate to introduce the alternating direction method of multipliers (ADMM) Boyd, Parikh, Chu, Peleato, Eckstein et al. (2011) when the loss function incorporates additional inequality and equality constraints. In addition, exploiting the correlation among labels or samples can increasingly boost the performance of LDL model. Jia et al. Jia et al. (2018) proposed LDLLC to take the global label correlation into account with introducing the Person's correlation between labels. It is pointed out in LDL-SCL Zheng, Jia and Li (2018) and EDL-LRL Jia et al. (2019b) that some correlations among labels (or samples) only exist in a set of instances, which are so-called the local correlation exploration. Intuitively, the instances in the same group after clustering share the same local correlation.

What's more, it is common that the labeled data are incomplete and contaminated Ma, Tian, Zhang and Chow (2017). For the former condition, Xu et al. Xu and Zhou (2017) put forward IncomLDL-a and IncomLDL-p on the assumption that the recovered complete label distribution matrix is low-rank. Proximal Gradient Descend (PGD) and ADMM are used for the optimization of two methods respectively. The time complexity of the first one is $O(1/T^2)$, and the last one is $O(1/T)$ but good at the accuracy. Jia et al. Jia, Ren, Chen, Wang, Zhu and Long (2019a) proposed WSLDL-MCSC which is based on the matrix completion and the exploration of samples' relevance in a transductive way when the data is under weak-supervision.

2.2. Label Enhancement Learning

To the best of our knowledge, there are a few researches whose topics focus on the label enhancement learning Xu et al. (2018). Five effective strategies have been devised during the present study. Four of them are adaptive algorithms. As discussed in Geng (2016), the concept of *membership* used in fuzzy clustering Jiang, Yi and Lv (2006) is similar to label distribution. Although they indicated two distinguishing semantics, they are both in numerical format. Thus, FCM El Gayar, Schwenker and Palm (2006) extend the calculation of membership which is used in fuzzy C-means clustering Melin and Castillo (2005) to recover the label distribution. LE algorithm based on kernel method (KM) Jiang et al. (2006) utilizes the kernel function to project the instances from origin space into a high-dimensional one. The instances are separated into two parts according to whether the corresponding logical label is 1 or not for every candidate label. Then the label distribution term, i.e. description degree can be calculated based on the distance between the instances and the center of groups. Label propagation technique Wang and Zhang (2007) is used in the LP method to update the label distribution matrix iteratively with a fully-connected graph built. Since the message between samples is shared and passed on the basis of the connection graph, the logical label can be enhanced into distribution-level label. LE method adapted from manifold learning (ML) Hou, Geng and Zhang (2016) take the topological consistency between feature space and label space into consideration to obtain the recovered label distribution. The last novel strategy called GLE Xu, Liu and Geng (2019a) is specialized by leveraging the topological information

Table 1
Summary of some notations

Notations	Description
n	the number of instances
c	number of labels
m	dimension of samples
X	instance feature matrix
L	logical label matrix
D	label distribution matrix
\hat{W}	Mapping parameter of BD-LE
\tilde{W}	Reconstruction parameter of BD-LE
θ	Mapping parameter of BD-LDL
$\tilde{\theta}$	Reconstruction parameter of BD-LDL

of the input space and the correlation among labels. Meanwhile, the local label correlation is captured via clustering Zhou, Zhang, Huang and Li (2012).

3. Proposed Method

Let $\mathcal{X} = \mathbb{R}^m$ denote the m -dimensional input space and $\mathcal{Y} = \{y_1, y_2, \dots, y_c\}$ represent the complete set of labels where c is the number of all possible labels. For each instance $x_i \in \mathcal{X}$, a simple logical label vector $l_i \in \{0, 1\}^c$ is leveraged to represent which labels can describe the instance correctly. Specially, for the LDL paradigm, instance x_i is assigned with distribution-level vector d_i

3.1. Bi-directional for Label Enhancement

Given a dataset $E = \{(x_1, l_1), (x_2, l_2), \dots, (x_n, l_n)\}$, $X = [x_1, x_2, x_3, \dots, x_n]$ and $L = [l_1, l_2, l_3, \dots, l_n]$ is defined as input matrix and logical label matrix, respectively. According to previous discussion, the goal of LE is to transform L into the label distribution matrix $D = [d_1, d_2, d_3, \dots, d_n]$.

Firstly, a nonlinear function $\varphi(\cdot)$, i.e., kernel function is defined to transform each instance x_i into a higher dimensional feature $\varphi(x_i)$, which can be utilized to construct the vector $\phi_i = [\varphi(x_i); 1]$ of corresponding instance. For each instance, an appropriate mapping parameter \hat{W} is required to transform the input feature ϕ_i into the label distribution d_i . As there is a large dimension gap between input space and output space, a lot of information may be lost during the mapping process. To address this issue, it is reasonable to introduce the parameter \tilde{W} for the reconstruction of the input data from the output data. Accordingly, the objective function of LE is formulated as follows:

$$\min_{\hat{W}, \tilde{W}} L(\hat{W}) + \alpha R(\tilde{W}) + \frac{1}{2} \lambda \Omega(\hat{W}) + \frac{1}{2} \lambda \Omega(\tilde{W}) \quad (1)$$

where L denotes the loss function of data mapping, R indicates the loss function of data reconstruction, Ω is the regularization term, λ and α are two trade-off parameters. It should be noted that the LE algorithm is regarded as a pre-processing of LDL methods and it dose not suffer from the over-fitting problem. Accordingly, it is not necessary to add the norm of parameters \hat{W} and \tilde{W} as regularizers.

The first term L is the mapping loss function to measure the distance between logical label and recovered label distribution. According to Xu et al. (2018), it is reasonable to select the least squared (LS) function:

$$\begin{aligned} L(\hat{W}) &= \sum_{i=1}^n \|\hat{W} \phi_i - l_i\|^2 \\ &= \text{tr} [(\hat{W} \Phi - L)^T (\hat{W} \Phi - L)] \end{aligned} \quad (2)$$

where $\Phi = [\phi_1, \dots, \phi_n]$ and $\text{tr}(\cdot)$ is the trace of a matrix defined by the sum of diagonal elements. The second term R is the reconstruction loss function to measure the similarity between the input feature data and the reconstructed one

from the output data of LE. Similar to the mapping loss function, the reconstruction loss function is defined as follows:

$$\begin{aligned} R(\tilde{W}) &= \sum_{i=1}^n \|\phi_i - \tilde{W}l_i\|^2 \\ &= \text{tr} [(\Phi - \tilde{W}L)^T (\Phi - \tilde{W}L)] \end{aligned} \quad (3)$$

To further simplify the model, it is reasonable to consider the tied weights Boureau, Cun et al. (2008) as follows:

$$\tilde{W}^* = \hat{W}^T \quad (4)$$

where \tilde{W}^* is the best reconstruction parameter to be obtained. Then the Eq. (1) is rewritten as:

$$\min_{\hat{W}} L(\hat{W}) + \alpha R(\hat{W}) + \lambda \Omega(\hat{W}) \quad (5)$$

To obtain desired results, the manifold regularization Ω is designed to capture the topological consistency between feature space and label space, which can fully exploit the hidden label importance from the input instances. Before presenting this term, it is required to introduce the similarity matrix A , whose element is defined as:

$$a_{ij} = \begin{cases} \exp\left(-\frac{\|x_i - x_j\|^2}{2\sigma^2}\right) & \text{if } x_j \in N(i) \\ 0 & \text{otherwise} \end{cases} \quad (6)$$

where $N(i)$ denotes the set of K -nearest neighbors for the instance x_i , and $\sigma > 0$ is the hyper parameter fixed to be 1 in this paper. Inspired by the smoothness assumption Zhu, Lafferty and Rosenfeld (2005), the more correlated two instances are, the closer are the corresponding recovered label distribution, and vice versa. Accordingly, it is reasonable to design the following manifold regularization:

$$\begin{aligned} \Omega(\hat{W}) &= \sum_{i,j} a_{ij} \|d_i - d_j\|^2 = \text{tr}(DGD^T) \\ &= \text{tr}(\hat{W}\Phi G\Phi^T \hat{W}^T) \end{aligned} \quad (7)$$

where $d_i = \hat{W}\phi_i$ indicates the recovered label distribution, and $G = \hat{A} - A$ is the Laplacian matrix. Note that the similarity matrix A is asymmetric so that the element of diagonal matrix \hat{A} element is defined as $\hat{a}_{ii} = \sum_{j=1}^n (a_{ij} + a_{ji})/2$,

By substituting Eqs. (2), (3) and (7) into Eq. (5), the mapping and reconstruction loss function is defined on parameter \hat{W} as follows:

$$\begin{aligned} T(\hat{W}) &= \text{tr}((\hat{W}\Phi - L)^T (\hat{W}\Phi - L)) \\ &+ \alpha \text{tr}((\Phi - \hat{W}^T L)^T (\Phi - \hat{W}^T L)) \\ &+ \lambda \text{tr}(\hat{W}\Phi G\Phi^T \hat{W}^T) \end{aligned} \quad (8)$$

Actually, Eq.(8) can be easily optimized by a well-known method called limited-memory quasi-Newton method (L-BFGS) Yuan (1991). This method achieves the optimization by calculating the first-order gradient of $T(\hat{W})$:

$$\begin{aligned} \frac{\partial T}{\partial \hat{W}} &= 2\hat{W}\Phi\Phi^T - 2L\Phi^T - 2\alpha L\Phi^T + 2\alpha LL^T \hat{W} \\ &+ \lambda \hat{W}\Phi G^T \Phi^T + \lambda \hat{W}\Phi G\Phi^T \end{aligned} \quad (9)$$

3.2. Bi-directional for Label Distribution Learning

Given dataset $S = \{(x_1, d_1), (x_2, d_2), \dots, (x_n, d_n)\}$ whose label is the real-valued format, LDL aims to build a mapping function $f: \mathcal{X} \rightarrow \mathcal{D}$ from the instances to the label distributions, where $x_i \in \mathcal{X}$ denotes the i -th instance and $d_i = \{d_{x_i}^{y_1}, d_{x_i}^{y_2}, \dots, d_{x_i}^{y_c}\} \in \mathcal{D}$ indicates the i -th label distribution of instance. Note that d_x^y accounts for the description

degree of y to x rather than the probability that label tags correctly. All the labels can describe each instance completely, so it is reasonable that $d_x^y \in [0, 1]$ and $\sum_y d_x^y = 1$.

As mentioned before, most of LDL methods suffer from the mapping information loss due to the unidirectional projection of loss function. Fortunately, bidirectional projections can extremely preserve the information of input matrix. Accordingly, the goal of our specific BD-LDL algorithm is to determine a mapping parameter θ and a reconstruction parameter $\tilde{\theta}$ from training set so as to make the predicted label distribution and the true one as similar as possible. Therefore, the new loss function integrates the mapping error with the reconstruction error $R(\tilde{\theta}, S)$ as follows:

$$\min_{\theta, \tilde{\theta}} L(\theta, S) + \lambda_1 R(\tilde{\theta}, S) + \frac{1}{2} \lambda_2 \Omega(\theta, S) + \frac{1}{2} \lambda_2 \Omega(\tilde{\theta}, S) \quad (10)$$

where θ denotes the mapping parameter, $\tilde{\theta}$ indicates the reconstruction parameter, Ω is a regularization to control the complexity of the output model to avoid over-fitting, λ_1 and λ_2 are two parameters to balance these four terms.

There are various candidate functions to measure the difference between two distributions such as the Euclidean distance, the Kullback-Leibler (K-L) divergence and the Clark distance etc. Here, we choose the Euclidean distance:

$$L(\theta, S) = \|X\theta - D\|_F^2 \quad (11)$$

where $\theta \in \mathbb{R}^{d \times c}$ is the mapping parameter to be optimized, and $\|\cdot\|_F^2$ is the Frobenius norm of a matrix. For simplification, it is reasonable to consider tied weights Boureau et al. (2008) as follows:

$$\tilde{\theta}^* = \theta^T \quad (12)$$

Similarly, the objective function is simplified as follows:

$$\min_{\theta} L(\theta, S) + \lambda_1 R(\theta, S) + \lambda_2 \Omega(\theta, S) \quad (13)$$

where the term $R(\theta, S) = \|X - D\theta^T\|_F^2$ denotes the simplified reconstruction error. As for the second term in objective function, we adopt the F-norm to implement it:

$$\Omega(\theta, S) = \|\theta\|_F^2 \quad (14)$$

Substituting Eqs. (11) and (14) into Eq. (13) yields the objective function:

$$\min_{\theta} \|X\theta - D\|_F^2 + \lambda_1 \|X - D\theta^T\|_F^2 + \lambda_2 \|\theta\|_F^2 \quad (15)$$

Before optimization, the trace properties $\text{tr}(X) = \text{tr}(X^T)$ and $\text{tr}(D\theta^T) = \text{tr}(\theta D^T)$ are applied for the re-organization of objective function:

$$\min_{\theta} \|X\theta - D\|_F^2 + \lambda_1 \|X^T - \theta D^T\|_F^2 + \lambda_2 \|\theta\|_F^2. \quad (16)$$

Then, for optimization, we can simply take a derivative of Eq. (16) with respect to the parameter θ and set it zero:

$$X^T(X\theta - D) - \lambda_1 (X^T - \theta D^T) D + \lambda_2 \theta = 0 \quad (17)$$

Obviously, Eq. (17) can be transformed into the following equivalent formulation:

$$(X^T X + \lambda_2 I) \theta + \lambda_1 \theta D^T D = X^T D + \lambda_1 X^T D \quad (18)$$

Denote $A = X^T X + \lambda_2 I$, $B = \lambda_1 D^T D$ and $C = (1 + \lambda_1) X^T D$, Eq. (18) can be rewritten as the following formulation:

$$A\theta + \theta B = C \quad (19)$$

Algorithm 1 BD-LDL Algorithm

Require: X : $n \times d$ training feature matrix;
 D : $n \times c$ labeled distribution matrix;
Ensure: θ : $d \times c$ projection parameter
 1: Initial θ^0 , λ_1 , λ_2 and $t = 0$;
 2: **repeat**
 3: Compute A , B and C in Eq.(19)
 4: Perform Cholesky factorization to gain P and Q
 5: Perform SVD on P and Q
 6: Update $\tilde{\theta}^{t+1}$ via Eqs.(24) and (25)
 7: Update θ^{t+1} via Eqs.(26)
 8: **until** Stopping criterion is satisfied

Although Eq. (19) is the well-known Sylvester equation which can be solved by existing algorithm in MATLAB, the computational cost corresponding solution is not ideal. Thus, following Zhu, Suk, Wang, Lee and Shen (2017), we effectively solve Eq. (19) with Cholesky factorization Golub and Loan (1996) as well the Singular Value Decomposition (SVD). Firstly, two positive semi-definite matrix A and B can be factorized as:

$$\begin{aligned} A &= P^T \times P \\ B &= Q \times Q^T \end{aligned} \quad (20)$$

where P and Q are the triangular matrix which can be further decomposed via SVD as:

$$\begin{aligned} P &= U_1 \Sigma_1 V_1^T \\ Q &= U_2 \Sigma_2 V_2^T \end{aligned} \quad (21)$$

Substituting Eqs. (20) and (21) into Eq. (19) yields:

$$V_1 \Sigma_1^T U_1^T U_1 \Sigma_1 V_1^T \theta + \theta U_2 \Sigma_2 V_2^T V_2 \Sigma_2^T U_2^T = C \quad (22)$$

Since U_1 , U_2 , V_1 and V_2 are the unitray matrix, Eq. (22) can be rewritten as :

$$V_1 \Sigma_1^T \Sigma_1 V_1^T \theta + \theta U_2 \Sigma_2 \Sigma_2^T U_2^T = C \quad (23)$$

We multiplying V_1^T and U_2 to both sides of Eq. (23) to obtain the following equation:

$$\tilde{\Sigma}_1 \tilde{\theta} + \tilde{\theta} \tilde{\Sigma}_2 = E \quad (24)$$

where $\tilde{\Sigma}_1 = \Sigma_1^T \Sigma_1$, $\tilde{\Sigma}_2 = \Sigma_2 \Sigma_2^T$, $E = V_1^T C U_2$ and $\tilde{\theta} = V_1^T \theta U_2$.

For both $\tilde{\Sigma}_1$ and $\tilde{\Sigma}_2$ are the diagonal matrix, we can directly attain $\tilde{\theta}$ whose element is defined as:

$$\tilde{\theta}_{ij} = \frac{e_{ij}}{\tilde{\sigma}_{ii}^1 + \tilde{\sigma}_{jj}^2} \quad (25)$$

where $\tilde{\sigma}_{ii}^1$ and $\tilde{\sigma}_{jj}^2$ can be calculated by eigenvalues of P and Q respectively, and e_{ij} is the i,j -th elment of matrix E . Accordingly, θ can be obtained by:

$$\theta = V_1 \tilde{\theta} U_2^T \quad (26)$$

We briefly summarize the procedure of the proposed BD-LDL in Algorithm 1.

Table 2

Statistics of 13 datasets used in comparison experiment

Index	Data Set	# Examples	# Features	# Labels
1	Yeast-alpha	2,465	24	18
2	Yeast-cdc	2,465	24	15
3	Yeast-cold	2,465	24	4
4	Yeast-diau	2,465	24	7
5	Yeast-dtt	2,465	24	4
6	Yeast-elu	2,465	24	14
7	Yeast-heat	2,465	24	6
8	Yeast-spo	2,465	24	6
9	Yeast-spo5	2,465	24	3
10	Yeast-spoem	2,465	24	2
11	Natural Scene	2,000	294	9
12	Movie	7,755	1,869	5
13	SBU_3DFE	2,500	243	6

Table 3

Evaluation Measurements

	Name	Defination
Distance	Chebyshev ↓	$Dis_1(D, \hat{D}) = \max_i d_i - \hat{d}_i $
	Clark ↓	$Dis_2(D, \hat{D}) = \sqrt{\sum_{i=1}^c \frac{(d_i - \hat{d}_i)^2}{(d_i + \hat{d}_i)^2}}$
	Canberra ↓	$Dis_3(D, \hat{D}) = \sum_{i=1}^c \frac{ d_i - \hat{d}_i }{d_i + \hat{d}_i}$
Similarity	Intersaction ↑	$Sim_1(D, \hat{D}) = \sum_{i=1}^c \min(d_i, \hat{d}_i)$
	Cosine ↑	$Sim_2(D, \hat{D}) = \frac{\sum_{i=1}^c d_i \hat{d}_i}{\sqrt{(\sum_{i=1}^c d_i^2)(\sum_{i=1}^c \hat{d}_i^2)}}$

4. Experiments

4.1. Datasets and Measurement

We conducted extensive experiments on 13 real-world datasets collected from biological experiments Eisen, Spellman, Brown and Botstein (1998), facial expression images Lyons, Akamatsu, Kamachi and Gyoba (1998), natural scene images, and movies. The output of both LE and LDL are in the format of label distribution vectors. In contrast to the results of SLL and MLL, the label distribution vectors should be evaluated with diverse measurements. We naturally select six criteria that are most commonly used, i.e., Chebyshev distance (Chebyshev), Clark distance (Clark), Canberra metric (Canberra), Kullback-Leibler divergence (K-L), Cosine coefficient (Cosine), and Intersection similarity (Intersec). The first four functions are always used to measure distance between ground-truth label distribution D and the predicted one \hat{D} , whereas the last two are similarity measurements. The specifications of criteria and used data sets can be found in Tables 3 and 2.

4.2. Methodology

To show the effectiveness of the proposed methods, we conducted comprehensive experiments on the aforementioned datasets. For LE, the proposed BD-LE method is compared with five classical LE approaches presented in Xu et al. (2018), i.e., FCM, KM, LP, ML, and GLLE. The hyper-parameter in the FCM method is set to 2. We select the Gaussian Kernel as the kernel function in the KM algorithm. For GLLE, the parameter λ is set to 0.01. Moreover, the number of neighbors K is set to $c + 1$ in both GLLE and ML.

For the LDL paradigm, the proposed BD-LDL method is compared with eight existing algorithms including PT-

Table 4

Comparison Performance(rank) of Different LE Algorithms Measured by Chebyshev ↓

Datasets	Ours	FCM	KM	LP	ML	GLLE
Yeast-alpha	0.0208(1)	0.0426(4)	0.0588(6)	0.0401(3)	0.0553(5)	0.0310(2)
Yeast-cdc	0.0231(1)	0.0513(4)	0.0729(6)	0.0421(3)	0.0673(5)	0.0325(2)
Yeast-cold	0.0690(1)	0.1325(4)	0.2522(6)	0.1129(3)	0.2480(5)	0.0903(2)
Yeast-diau	0.0580(1)	0.1248(4)	0.2500(6)	0.0904(3)	0.1330(5)	0.0789(2)
Yeast-dtt	0.0592(1)	0.0932(3)	0.2568(5)	0.1184(4)	0.2731(6)	0.0651(2)
Yeast-elu	0.0256(1)	0.0512(4)	0.0788(6)	0.0441(3)	0.0701(5)	0.0287(2)
Yeast-heat	0.0532(1)	0.1603(4)	0.1742(5)	0.0803(3)	0.1776(6)	0.0563(2)
Yeast-spo	0.0641(1)	0.1300(4)	0.1753(6)	0.0834(3)	0.1722(5)	0.0670(2)
Yeast-spo5	0.1017(2)	0.1622(4)	0.2773(6)	0.1142(3)	0.2730(5)	0.0980(1)
Yeast-spoem	0.0921(1)	0.2333(4)	0.4006(6)	0.1632(3)	0.3974(5)	0.1071(2)
Natural_Scene	0.3355(5)	0.3681(6)	0.3060(3)	0.2753(1)	0.2952(2)	0.3349(4)
Movie	0.1254(1)	0.2302(4)	0.2340(6)	0.1617(3)	0.2335(5)	0.1601(2)
SUB_3DFE	0.1285(1)	0.1356(3)	0.2348(6)	0.1293(2)	0.2331(5)	0.1412(4)
Avg. Rank	1.38	4.00	5.62	2.84	4.92	2.23

Table 5

Comparison Performance(rank) of Different LE Algorithms Measured by Cosine ↑

Datasets	Ours	FCM	KM	LP	ML	GLLE
Yeast-alpha	0.9852(1)	0.9221(3)	0.8115(5)	0.9220(4)	0.7519(6)	0.9731(2)
Yeast-cdc	0.9857(1)	0.9236(3)	0.7541(6)	0.9162(4)	0.7591(5)	0.9597(2)
Yeast-cold	0.9804(1)	0.9220(4)	0.7789(6)	0.9251(3)	0.7836(5)	0.9690(2)
Yeast-diau	0.9710(1)	0.8901(4)	0.7990(6)	0.9153(3)	0.8032(5)	0.9397(2)
Yeast-dtt	0.9847(1)	0.9599(3)	0.7602(6)	0.9210(4)	0.7631(5)	0.9832(2)
Yeast-elu	0.9841(1)	0.9502(3)	0.7588(5)	0.9110(4)	0.7562(6)	0.9813(2)
Yeast-heat	0.9803(1)	0.8831(4)	0.7805(6)	0.9320(3)	0.7845(5)	0.9800(2)
Yeast-spo	0.9719(1)	0.9092(4)	0.8001(6)	0.9390(3)	0.8033(5)	0.9681(2)
Yeast-spo5	0.9697(2)	0.9216(4)	0.8820(6)	0.9694(3)	0.8841(5)	0.9713(1)
Yeast-spoem	0.9761(1)	0.8789(4)	0.8122(6)	0.9500(3)	0.8149(5)	0.9681(2)
Natural_Scene	0.7797(4)	0.5966(6)	0.7488(5)	0.8602(2)	0.8231(1)	0.7822(3)
Movie	0.9321(1)	0.7732(6)	0.8902(4)	0.9215(2)	0.8153(5)	0.9000(3)
SBU_3DFE	0.9233(1)	0.9117(3)	0.8126(6)	0.9203(2)	0.8150(5)	0.9000(4)
Avg. Rank	1.31	3.92	5.62	3.08	4.85	2.23

Bayes Geng and Ji (2013), PT-SVM Geng et al. (2014), AA-KNN Geng et al. (2010), AA-BP Geng et al. (2013), SA-IIS Geng et al. (2013), SA-BFGS Geng (2016), LDL-SCL Zheng et al. (2018), and EDL-LRL Jia et al. (2019b), to demonstrate its superiority. The first two algorithms are implemented by the strategy of problem transformation. The next two ones are carried out by means of the adaptive method. Finally, from the fifth algorithm to the last one, they are specialized algorithms. In particular, the LDL-SCL and EDL-LRL constitute state-of-art methods recently proposed. We utilized the “C-SVC” type in LIBSVM to implement PT-SVM using the RBF kernel with parameters $C = 10^{-1}$ and $\gamma = 10^{-2}$. We set the hyper-parameter k in AA-kNN to 5. The number of hidden-layer neurons for AA-BP was set to 60. The parameters λ_1 , λ_2 and λ_3 in LDL-SCL were all set to 10^{-3} . Regarding the EDL-LRL algorithm, we set the regularization parameters λ_1 and λ_2 to 10^{-3} and 10^{-2} , respectively. For the intermediate algorithm K-means, the number of cluster was set to 5 according to Jia’s suggestion Jia et al. (2018). For the BFGS optimization used in SA-BFGS and BD-LDL, parameters c_1 and c_2 were set to 10^{-4} and 0.9, respectively. Regarding the two bi-directional algorithms, parameters are tuned from the range $10^{\{-4, -3, -2, -1, 0, 1, 2, 3\}}$ using grid-search method. The two parameters in BD-LE α and λ are both set to 10^{-3} . As for BD-LDL, the parameters λ_1 and λ_2 are set to 10^{-3} and 10^{-2} , respectively. Finally, we train the LDL model with the recovered label distributions for further evaluation of BD-LE. The details

Table 6

 Comparison Results(mean \pm std.(rank)) of Different LDL Algorithms Measured by Clark \downarrow

Datasets	Ours	PT-Bayes	AA-BP	SA-IIS	SA-BFGS	LDL-SCL	EDL-LRL	LDLLC
Yeast-alpha	0.2097\pm0.003(1)	1.1541 \pm 0.034(8)	0.7236 \pm 0.060(7)	0.3053 \pm 0.006(6)	0.2689 \pm 0.008(5)	0.2098 \pm 0.002(2)	0.2126 \pm 0.000(4)	0.2098 \pm 0.006(3)
Yeast-cdc	0.2017\pm0.004(1)	1.0601 \pm 0.066(8)	0.5728 \pm 0.030(7)	0.2932 \pm 0.004(6)	0.2477 \pm 0.007(5)	0.2137 \pm 0.004(3)	0.2046 \pm 2.080(2)	0.2163 \pm 0.004(4)
Yeast-cold	0.1355\pm0.004(1)	0.5149 \pm 0.024(8)	0.1552 \pm 0.005(7)	0.1643 \pm 0.004(8)	0.1471 \pm 0.004(5)	0.1388 \pm 0.003(2)	0.1442 \pm 2.100(4)	0.1415 \pm 0.004(3)
Yeast-diau	0.1960\pm0.006(1)	0.7487 \pm 0.042(8)	0.2677 \pm 0.010(7)	0.2409 \pm 0.006(6)	0.2201 \pm 0.002(5)	0.1986 \pm 0.002(2)	0.2011 \pm 0.003(4)	0.2010 \pm 0.006(3)
Yeast-dtt	0.0964 \pm 0.004(2)	0.4807 \pm 0.040(8)	0.1206 \pm 0.008(7)	0.1332 \pm 0.003(8)	0.1084 \pm 0.003(6)	0.0989 \pm 0.001(4)	0.0980 \pm 1.600(3)	0.0962\pm0.006(1)
Yeast-elu	0.1964\pm0.004(1)	1.0050 \pm 0.041(8)	0.5246 \pm 0.028(7)	0.2751 \pm 0.006(6)	0.2438 \pm 0.008(5)	0.2015 \pm 0.002(3)	0.2029 \pm 0.023(4)	0.1994 \pm 0.006(2)
Yeast-heat	0.1788\pm0.005(1)	0.6829 \pm 0.026(8)	0.2261 \pm 0.010(7)	0.2260 \pm 0.005(6)	0.1998 \pm 0.003(5)	0.1826 \pm 0.003(2)	0.1826 \pm 0.003(2)	0.1854 \pm 0.004(4)
Yeast-spo	0.2456\pm0.008(1)	0.6686 \pm 0.040(8)	0.2950 \pm 0.010(7)	0.2759 \pm 0.006(6)	0.2639 \pm 0.003(5)	0.2503 \pm 0.002(4)	0.2480 \pm 0.685(2)	0.2500 \pm 0.008(3)
Yeast-spo5	0.1785\pm0.007(1)	0.4220 \pm 0.020(8)	0.1870 \pm 0.005(3)	0.1944 \pm 0.009(6)	0.1962 \pm 0.001(7)	0.1881 \pm 0.004(4)	0.1915 \pm 0.020(5)	0.1837 \pm 0.007(2)
Yeast-spoem	0.1232\pm0.005(1)	0.3065 \pm 0.030(8)	0.1890 \pm 0.012(7)	0.1367 \pm 0.007(6)	0.1312 \pm 0.001(3)	0.1316 \pm 0.005(4)	0.1273 \pm 0.054(2)	0.1320 \pm 0.008(5)
Natural_Scene	2.3612\pm0.541(1)	2.5259 \pm 0.015(8)	2.4534 \pm 0.018(4)	2.4703 \pm 0.019(6)	2.4754 \pm 0.013(7)	2.4580 \pm 0.012(5)	2.4519 \pm 0.005(2)	2.4456 \pm 0.019(3)
Movie	0.5211\pm0.606(1)	0.8044 \pm 0.010(8)	0.6533 \pm 0.010(6)	0.5783 \pm 0.007(5)	0.5750 \pm 0.011(4)	0.5543 \pm 0.007(3)	0.6956 \pm 0.041(7)	0.5289 \pm 0.008(2)
SBU_3DFE	0.3540 \pm 0.010(2)	0.4137 \pm 0.010(5)	0.4454 \pm 0.020(8)	0.4156 \pm 0.012(7)	0.3465\pm0.006(1)	0.3546 \pm 0.002(3)	0.3556 \pm 0.006(4)	0.4145 \pm 0.006(6)
Avg. Rank	1.15	7.77	6.46	6.31	4.85	3.15	3.46	3.15

Table 7

 Comparison Results(mean \pm std.(rank)) of Different LDL Algorithms Measured by Cosine \uparrow

Datasets	Ours	PT-Bayes	AA-BP	SA-IIS	SA-BFGS	LDL-SCL	EDL-LRL	LDLLC
Yeast-alpha	0.9947\pm0.000(1)	0.8527 \pm 0.005(8)	0.9482 \pm 0.007(7)	0.9879 \pm 0.000(6)	0.9914 \pm 0.000(5)	0.9945 \pm 0.000(3)	0.9945 \pm 0.000(4)	0.9946 \pm 0.000(2)
Yeast-cdc	0.9955\pm0.000(1)	0.8544 \pm 0.012(8)	0.9590 \pm 0.003(7)	0.9871 \pm 0.000(6)	0.9913 \pm 0.000(4)	0.9904 \pm 0.000(5)	0.9939 \pm 8.070(2)	0.9932 \pm 0.000(3)
Yeast-cold	0.9893\pm0.001(1)	0.8884 \pm 0.008(8)	0.9859 \pm 0.001(6)	0.9838 \pm 0.000(7)	0.9871 \pm 0.000(5)	0.9886 \pm 0.000(3)	0.9892 \pm 0.034(2)	0.9883 \pm 0.001(4)
Yeast-diau	0.9884\pm0.001(1)	0.8644 \pm 0.007(8)	0.9860 \pm 0.000(5)	0.9821 \pm 0.000(7)	0.9853 \pm 0.000(6)	0.9880 \pm 0.000(2)	0.9876 \pm 0.063(4)	0.9878 \pm 0.001(3)
Yeast-dtt	0.9943\pm0.000(1)	0.8976 \pm 0.012(8)	0.9909 \pm 0.001(6)	0.9889 \pm 0.000(7)	0.9928 \pm 0.000(5)	0.9939 \pm 0.000(3)	0.9940 \pm 0.021(2)	0.9939 \pm 0.001(4)
Yeast-elu	0.9942\pm0.000(1)	0.8600 \pm 0.008(8)	0.9623 \pm 0.003(7)	0.9876 \pm 0.000(6)	0.9912 \pm 0.000(5)	0.9939 \pm 0.000(3)	0.9938 \pm 0.001(4)	0.9940 \pm 0.000(2)
Yeast-heat	0.9884\pm0.001(1)	0.8655 \pm 0.008(8)	0.9814 \pm 0.001(6)	0.9810 \pm 0.000(7)	0.9857 \pm 0.000(5)	0.9880 \pm 0.000(2)	0.9880 \pm 0.029(3)	0.9876 \pm 0.001(4)
Yeast-spo	0.9776\pm0.001(1)	0.8672 \pm 0.010(8)	0.9686 \pm 0.003(7)	0.9718 \pm 0.001(6)	0.9745 \pm 0.000(5)	0.9768 \pm 0.000(4)	0.9772 \pm 0.010(2)	0.9770 \pm 0.001(3)
Yeast-spo5	0.9753\pm0.002(1)	0.8968 \pm 0.010(8)	0.9731 \pm 0.001(4)	0.9706 \pm 0.002(7)	0.9710 \pm 0.000(6)	0.9732 \pm 0.001(3)	0.9723 \pm 0.007(5)	0.9743 \pm 0.002(2)
Yeast-spoem	0.9803\pm0.001(1)	0.9187 \pm 0.010(8)	0.9728 \pm 0.003(7)	0.9764 \pm 0.001(6)	0.9786 \pm 0.000(3)	0.9784 \pm 0.001(4)	0.9796 \pm 0.008(2)	0.9784 \pm 0.002(5)
Natural_Scene	0.7637\pm0.015(1)	0.5583 \pm 0.006(8)	0.6954 \pm 0.014(7)	0.6986 \pm 0.008(6)	0.7144 \pm 0.008(5)	0.7442 \pm 0.007(3)	0.7624 \pm 0.003(2)	0.7486 \pm 0.014(4)
Movie	0.9385\pm0.002(1)	0.8495 \pm 0.003(8)	0.8767 \pm 0.006(7)	0.9089 \pm 0.002(4)	0.8780 \pm 0.004(5)	0.9205 \pm 0.002(3)	0.8780 \pm 0.005(6)	0.9381 \pm 0.003(2)
SUB_3DFE	0.9644\pm0.004(1)	0.9167 \pm 0.004(8)	0.9181 \pm 0.005(7)	0.9202 \pm 0.004(5)	0.9482 \pm 0.001(3)	0.9436 \pm 0.000(4)	0.9636 \pm 0.002(2)	0.9198 \pm 0.002(6)
Avg. Rank	1.00	8.00	6.38	6.15	4.77	3.54	3.08	3.38

of parameter selections are shown in the parameter analysis section. And the experiments for the LDL algorithm on every datasets are conducted on a ten-fold cross-validation.

4.3. Results

4.3.1. BD-LE performance

Tables 1 and 2 present the results of six LE methods on all the datasets. Constrained by the page limit, we have only shown two representative results measured on Chebyshev and Cosine in this paper.

For each dataset, the results made by a specific algorithm are listed as a column in the tables in accordance with the used matrix. Note that there is always an entry highlighted in boldface. This entry indicates that the algorithm evaluated by the corresponding measurement achieves the best performance. The experimental results are presented in the form of “score (rank)”; “score” denotes the difference between a predicted distribution and the real one measured by the corresponding matrix; “rank” is a direct value to evaluate the effectiveness of these compared algorithms. Moreover, the symbol “ \downarrow ” means “the smaller the better”, whereas “ \uparrow ” indicates “the larger the better.”

It is worth noting that given that the LE method is regarded as a pre-processing method, there is no need to run it several times and record the mean as well as the standard deviation. After analyzing the results we obtained, the proposed BD-LE clearly outperforms other LE algorithms in most of the cases and renders sub-optimum performance only in about 4.7% of cases according to the statistics. In addition, BD-LE achieves better prediction results than GLLE in most of the cases, especially on dataset movie. From Table 1 we can see that the largest dimensional gap between input space and the output one is exactly in dataset movie. This indicates that the reconstruction projection can be added in LE algorithm reasonably. Two specialized algorithms, namely BE-LE and GLLE, rank first in 91.1% of cases. By contrast, the label distributions are hardly recovered from other four algorithms. This indicates the superiority of utilizing direct similarity or distance as the loss function in LDL and LE problems. In summary, the performance of the five LE algorithms is ranked from best to worst as follows: BD-LE, GLLE, LP, FCM, ML and KM. This proves the effectiveness of our proposed bi-directional loss function for the LE method.

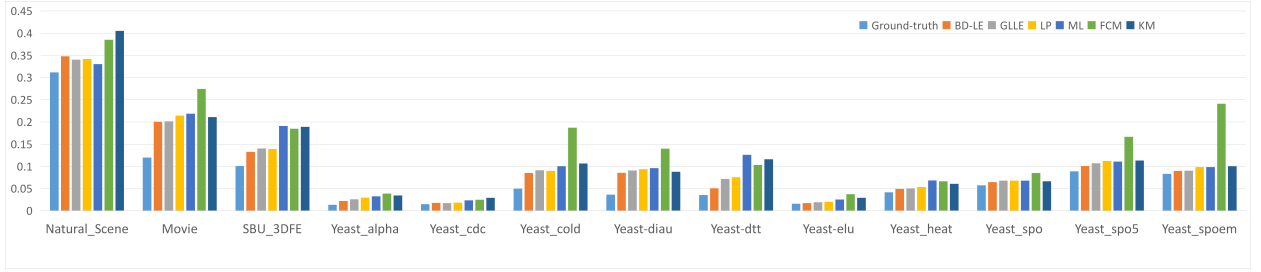


Figure 2: Comparison results of different LE algorithms against the “Ground-truth” used in BD-LDL measured by Chebyshev ↓

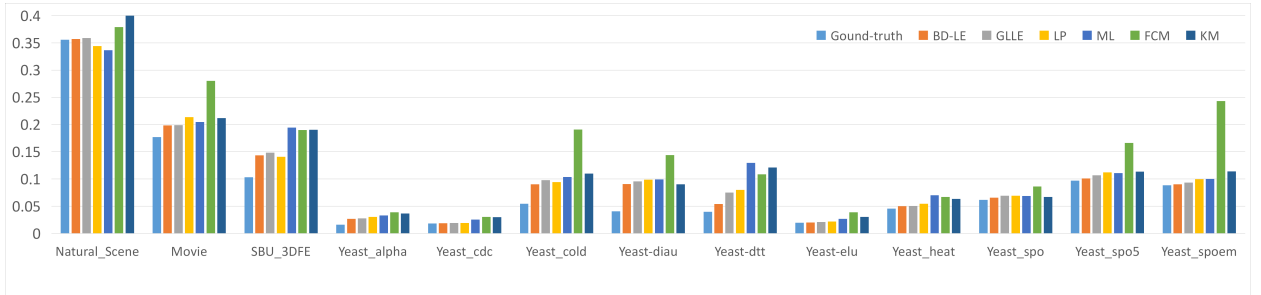


Figure 3: Comparison results of different LE algorithms against the “Ground-truth” used in SA-BFGS measured by Chebyshev ↓

4.3.2. BD-LDL performance

As for the performance of BD-LDL method, we show the numerical result on 13 real-world datasets over the measurement Clark and Cosine in Tables 3 and 4 with the format “mean±std (rank)” similarly, and the item in bold in every row represents the best performance. One may observe that our algorithm BD-LDL outperforms other classical LDL algorithms in most cases. When measured by Cosine, it is vividly shown that BD-LDL achieves the best performance on every datasets, which strongly demonstrates the effectiveness of our proposed method. Besides, it can be found from Table 4 that although LDLLC and SA-BFGS obtains the best result on dataset Yeast-dtt and SBU_3DFE respectively when measured with Chebyshev, BD-LDL still ranks the second place. It also can be seen from the results that two PT and AP algorithms perform poorly on most cases. This verifies the superiority of utilizing the direct similarity or distance between the predicted label distribution and the true one as the loss function. Moreover, it can be easily seen from the results that our proposed method gains the superior performance over other existing specialized algorithms which ignore considering the reconstruction error. This indicates that such a bi-directional loss function can truly boost the performance of LDL algorithm.

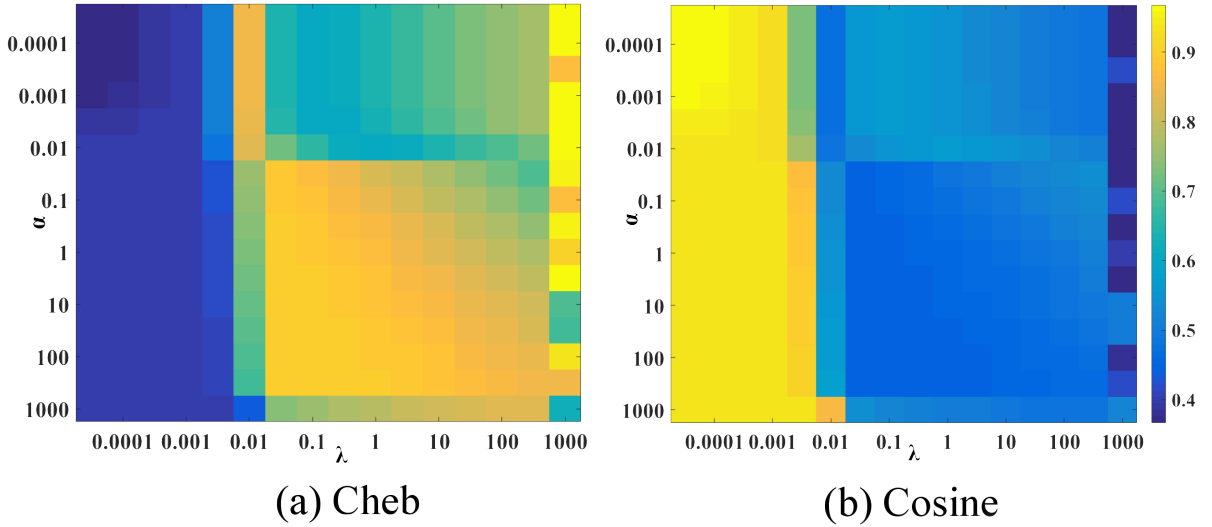
4.3.3. LDL algorithm Predictive Performance

The reason to use the LE algorithm is that we need to recover the label distributions for LDL training. For the purpose of verifying the correctness and effectiveness of our proposed LE algorithm, we conducted an experiment to compare predictions depending on the recovered label distributions with those made by the LDL model trained on real label distributions. Moreover, for further evaluation of the proposed BD-LDL, we selected BD-LDL and SA-BFGS as the LDL model in this experiment. Owing to the page limit, we hereby present only the experimental results measured with Chebyshev. The prediction results achieved from SA-BFGS and BD-LDL are visualized in Figs. 1 and 2 in terms of histograms. Note that ‘Ground-truth’ appearing in the figures represents the results depending on the real label distributions. We regard these results as a benchmark instead of taking them into consideration while conducting the evaluation. Meanwhile, we use ‘FCM’, ‘KM’, ‘LP’, ‘ML’, ‘GLLE’ and ‘BD-LE’ to represent the performance of the corresponding LE algorithm in this experiment. As illustrated in Figs. 1-2, although the prediction on datasets

Table 8

 Ablation experiments results of UD-LDL and BD-LDL Algorithms Measured by Canberra \downarrow and Intersection \uparrow

Dataset	Canberra \downarrow		Intersection \uparrow	
	UD-LDL	BD-LDL	UD-LDL	BD-LDL
Yeast-alpha	0.7980 \pm 0.013	0.6013\pm0.011	0.8915 \pm 0.001	0.9624\pm0.001
Yeast-cdc	0.9542 \pm 0.012	0.6078\pm0.012	0.8869 \pm 0.001	0.9580\pm0.001
Yeast-cold	0.4515 \pm 0.010	0.2103\pm0.007	0.8779 \pm 0.002	0.9430\pm0.002
Yeast-diau	0.6751 \pm 0.010	0.4220\pm0.013	0.8338 \pm 0.001	0.9414\pm0.002
Yeast-dtt	0.3724 \pm 0.010	0.1659\pm0.006	0.8775 \pm 0.002	0.9590\pm0.001
Yeast-elu	0.8005 \pm 0.007	0.5789\pm0.011	0.8776 \pm 0.001	0.9591\pm0.001
Yeast-heat	0.5706 \pm 0.010	0.3577\pm0.010	0.8591 \pm 0.002	0.9412\pm0.002
Yeast-spo	0.7075 \pm 0.016	0.5036\pm0.019	0.8301 \pm 0.003	0.9171\pm0.003
Yeast-spo5	0.4834 \pm 0.010	0.2745\pm0.011	0.8184 \pm 0.003	0.9112\pm0.003
Yeast-spoem	0.2998 \pm 0.010	0.1716\pm0.007	0.8129 \pm 0.005	0.9169\pm0.003
Natural_Scene	6.9653 \pm 0.095	0.7319\pm0.040	0.3822 \pm 0.010	0.5395\pm0.011
Movie	1.4259 \pm 0.024	0.0218\pm0.001	0.7429 \pm 0.004	0.8298\pm0.002
SBU_3DFE	0.8562 \pm 0.021	0.0119\pm0.001	0.8070 \pm 0.004	0.8590\pm0.004


Figure 4: Influence of parameter λ and α on dataset *cold* in BD-LE

movie and SUB_3DFE is worse than other datasets, ‘BD-LE’ is still relatively close to ‘Ground-Truth’ in most cases, especially in the first to eleventh datasets. We must mention that ‘BD-LE’ combined with BD-LDL is closer to ‘Ground-truth’ than with SA-BFGS over all cases. This indicates that such a reconstruction constraint is generalized enough to bring the improvement into both LE and LDL algorithms simultaneously.

4.4. Ablation Experiment

It is clear that the bi-directional loss for either LE or LDL consists of two parts, i.e., naive mapping loss and the reconstruction loss. In order to further demonstrate the effectiveness of the additional reconstruction term, we conduct the ablation experiment measured with Canberra and Intersection on the whole 13 datasets. We call the unidirectional

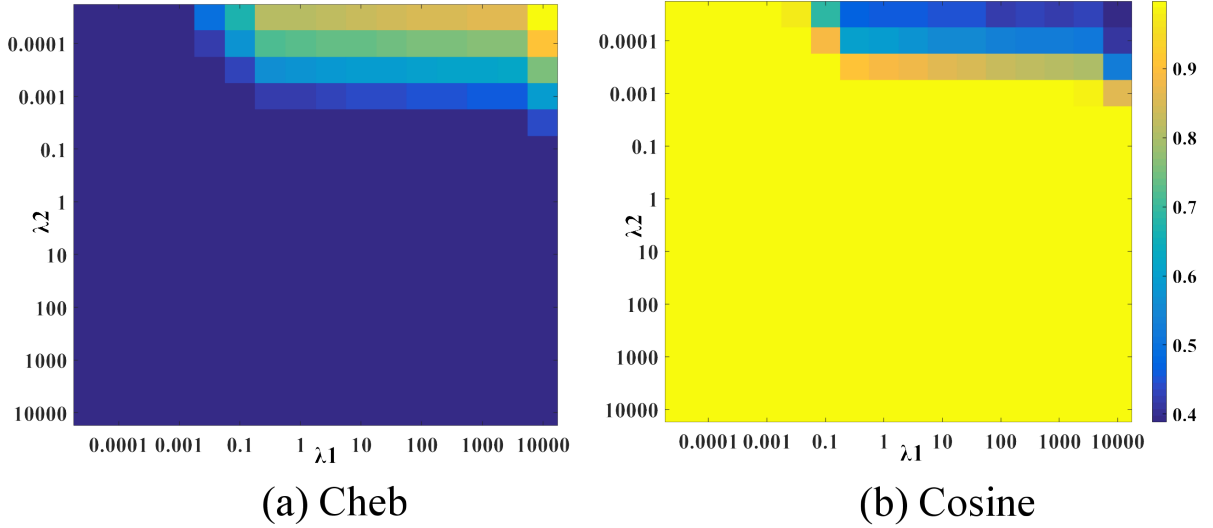


Figure 5: Influence of parameter λ_1 and λ_2 on dataset *cold* in BD-LDL

algorithm without reconstruction term as *UD-LE* and *UD-LE* respectively which are fomulated as:

$$\min_{\hat{W}} L(\hat{W}) + \Omega(W) \quad (27)$$

$$\min_{\theta} L(\theta, S) + \lambda \Omega(\theta, S) \quad (28)$$

Since the objective function of UD-LE is identical to that of GLLE, the corresponding comparison can be referred to Tables 2 and 3. The LDL prediction results in metrics of Canberra and Intersection are tabulated in Table 6.

From Table 6 we can see that BD-LDL gains the superior results in all benchmark datasets, i.e., introducing the reconstruction term can truly boost the performance of LDL algorithm. It is expected that the top-3 improvements are achieved in datasets Natural Scene, Movie, SBU_3DFE respectively which are equipped with the relative large dimensional gap between the feature and label space.

4.5. Influence of Parameters

To examine the robustness of the proposed algorithms, we also analyze the influence of trade-off parameters in the experiments, including λ_1 , λ_2 in BD-LDL as well as α and λ in BD-LE. We run BD-LE with α and λ whose value range is $[10^{-4}, 10^3]$, and parameters λ_1 and λ_2 involved in BD-LDL use the same candidate label set as well. Owing to the page limit, we only show in this paper the experimental results on Yeast-cold dataset which are measured with Chebyshev and Cosine. For further evaluation, the results are visualized with different colors in Figs. 5 and 6. When measured with Chebyshev, a smaller value means better performance and closer to blue; by contrast, with cosine, a larger value indicates better performance and closer to red.

It is clear from Fig. 5 that when λ falls in a certain range $[10^{-4}, 10^{-1}]$, we can achieve relatively good recovery results with any values of α . After conducting several experiments, we draw a conclusion for BD-LE, namely that when both α and λ are about 10^{-2} , the best performance is obtained. Concerning the parameters of BD-LDL, when the value of λ_1 is selected within the range $[10^{-1}, 10^3]$, the color varies in an extremely steady way, which means that the performance is not sensitive to this hyper parameter in that particular range. In addition, we can also see from Fig. 6 that λ_1 has a stronger influence on the performance than λ_2 when the value of λ_2 is within the range $[10^{-4}, 10^{-1}]$.

5. Conclusion

Previous studies have shown that the LDL method can effectively solve label ambiguity problems whereas the LE method is able to recover label distributions from logical labels. To improve the performance of LDL and LE methods, we propose a new loss function that combines the mapping error with the reconstruction error to leverage the missing information caused by the dimensional gap between the input space and the output one. Sufficient experiments have been conducted to show that the proposed loss function is sufficiently generalized for application in both LDL and LE with improvement. In the future, we will explore if there exists an end-to-end way to recover the label distributions with the supervision of LDL training process.

References

- Berger, A.L., Pietra, V.J.D., Pietra, S.A.D., 1996. A maximum entropy approach to natural language processing. *Computational linguistics* 22, 39–71.
- Boureau, Y.I., Cun, Y.L., et al., 2008. Sparse feature learning for deep belief networks, in: *Advances in neural information processing systems*, pp. 1185–1192.
- Boyd, S., Parikh, N., Chu, E., Peleato, B., Eckstein, J., et al., 2011. Distributed optimization and statistical learning via the alternating direction method of multipliers. *Foundations and Trends® in Machine learning* 3, 1–122.
- Cheng, Y., Zhao, D., Wang, Y., Pei, G., 2019. Multi-label learning with kernel extreme learning machine autoencoder. *Knowledge-Based Systems* 178, 1–10.
- Eisen, M.B., Spellman, P.T., Brown, P.O., Botstein, D., 1998. Cluster analysis and display of genome-wide expression patterns. *Proceedings of the National Academy of Sciences* 95, 14863–14868.
- El Gayar, N., Schwenker, F., Palm, G., 2006. A study of the robustness of knn classifiers trained using soft labels, in: *IAPR Workshop on Artificial Neural Networks in Pattern Recognition*, Springer. pp. 67–80.
- Fan, Y.Y., Liu, S., Li, B., Guo, Z., Samal, A., Wan, J., Li, S.Z., 2017. Label distribution-based facial attractiveness computation by deep residual learning. *IEEE Transactions on Multimedia* 20, 2196–2208.
- Geng, X., 2016. Label distribution learning. *IEEE Transactions on Knowledge and Data Engineering* 28, 1734–1748.
- Geng, X., Hou, P., 2015. Pre-release prediction of crowd opinion on movies by label distribution learning, in: *Twenty-Fourth International Joint Conference on Artificial Intelligence*.
- Geng, X., Ji, R., 2013. Label distribution learning, in: *Proceedings of the 2013 IEEE 13th International Conference on Data Mining Workshops*, IEEE Computer Society. pp. 377–383.
- Geng, X., Smith-Miles, K., Zhou, Z.H., 2010. Facial age estimation by learning from label distributions, in: *Proceedings of the Twenty-Fourth AAAI Conference on Artificial Intelligence*, AAAI Press. pp. 451–456.
- Geng, X., Wang, Q., Xia, Y., 2014. Facial age estimation by adaptive label distribution learning, in: *2014 22nd International Conference on Pattern Recognition*, IEEE. pp. 4465–4470.
- Geng, X., Yin, C., Zhou, Z.H., 2013. Facial age estimation by learning from label distributions. *IEEE transactions on pattern analysis and machine intelligence* 35, 2401–2412.
- Golub, G.H., Loan, C.F.V., 1996. *Matrix computations* (3rd ed.) .
- He, Z.F., Yang, M., Gao, Y., Liu, H.D., Yin, Y., 2019. Joint multi-label classification and label correlations with missing labels and feature selection. *Knowledge-Based Systems* 163, 145–158.
- Hou, P., Geng, X., Zhang, M.L., 2016. Multi-label manifold learning, in: *Thirtieth AAAI Conference on Artificial Intelligence*.
- Jia, X., Li, W., Liu, J., Zhang, Y., 2018. Label distribution learning by exploiting label correlations, in: *Thirty-Second AAAI Conference on Artificial Intelligence*.
- Jia, X., Ren, T., Chen, L., Wang, J., Zhu, J., Long, X., 2019a. Weakly supervised label distribution learning based on transductive matrix completion with sample correlations. *Pattern Recognition Letters* 125, 453–462.
- Jia, X., Zheng, X., Li, W., Zhang, C., Li, Z., 2019b. Facial emotion distribution learning by exploiting low-rank label correlations locally, in: *Proceedings of the IEEE Conference on Computer Vision and Pattern Recognition*, pp. 9841–9850.
- Jiang, X., Yi, Z., Lv, J.C., 2006. Fuzzy svm with a new fuzzy membership function. *Neural Computing & Applications* 15, 268–276.
- Kodirov, Elyor, X.T., Gong, S., 2017. Semantic autoencoder for zero-shot learning, in: *Proceedings of the IEEE Conference on Computer Vision and Pattern Recognition*, pp. 3174–3183.
- Lyons, M., Akamatsu, S., Kamachi, M., Gyoba, J., 1998. Coding facial expressions with gabor wavelets, in: *Proceedings Third IEEE international conference on automatic face and gesture recognition*, IEEE. pp. 200–205.
- Ma, J., Tian, Z., Zhang, H., Chow, T.W., 2017. Multi-label low-dimensional embedding with missing labels. *Knowledge-Based Systems* 137, 65–82.
- Malouf, R., 2002. A comparison of algorithms for maximum entropy parameter estimation, in: *proceedings of the 6th conference on Natural language learning-Volume 20*, Association for Computational Linguistics. pp. 1–7.
- Melin, P., Castillo, O., 2005. Hybrid intelligent systems for pattern recognition using soft computing: An evolutionary approach for neural networks and fuzzy systems. volume 172. Springer Science & Business Media.
- Nocedal, J., Wright, S., 2006. Numerical optimization. Springer Science & Business Media.
- Ren, T., Jia, X., Li, W., Chen, L., Li, Z., 2019a. Label distribution learning with label-specific features., in: *Proceedings of the 28th International Joint Conference on Artificial Intelligence*, pp. 3318–3324.

- Ren, T., Jia, X., Li, W., Zhao, S., 2019b. Label distribution learning with label correlations via low-rank approximation, in: Proceedings of the 28th International Joint Conference on Artificial Intelligence, AAAI Press. pp. 3325–3331.
- Tsoumakas, G., Katakis, I., 2007. Multi-label classification: An overview. International Journal of Data Warehousing and Mining (IJDWM) 3, 1–13.
- Wang, F., Zhang, C., 2007. Label propagation through linear neighborhoods. IEEE Transactions on Knowledge and Data Engineering 20, 55–67.
- Xing, C., Geng, X., Xue, H., 2016. Logistic boosting regression for label distribution learning, in: Proceedings of the IEEE conference on computer vision and pattern recognition, pp. 4489–4497.
- Xu, M., Zhou, Z.H., 2017. Incomplete label distribution learning., in: IJCAI, pp. 3175–3181.
- Xu, N., Liu, Y.P., Geng, X., 2019a. Label enhancement for label distribution learning. IEEE Transactions on Knowledge and Data Engineering .
- Xu, N., Lv, J., Geng, X., 2019b. Partial label learning via label enhancement.
- Xu, N., Tao, A., Geng, X., 2018. Label enhancement for label distribution learning., in: IJCAI, pp. 2926–2932.
- Xu, S., Shang, L., Shen, F., 2019c. Latent semantics encoding for label distribution learning., in: Proceedings of the 28th International Joint Conference on Artificial Intelligence, pp. 3982–3988.
- Xu, S., Yang, X., Yu, H., Yu, D.J., Yang, J., Tsang, E.C., 2016. Multi-label learning with label-specific feature reduction. Knowledge-Based Systems 104, 52–61.
- Yuan, Y.x., 1991. A modified bfgs algorithm for unconstrained optimization. IMA Journal of Numerical Analysis 11, 325–332.
- Zheng, X., Jia, X., Li, W., 2018. Label distribution learning by exploiting sample correlations locally, in: Thirty-Second AAAI Conference on Artificial Intelligence.
- Zhou, Y., Xue, H., Geng, X., 2015. Emotion distribution recognition from facial expressions, in: Proceedings of the 23rd ACM international conference on Multimedia, ACM. pp. 1247–1250.
- Zhou, Z.H., Zhang, M.L., Huang, S.J., Li, Y.F., 2012. Multi-instance multi-label learning. Artificial Intelligence 176, 2291–2320.
- Zhu, X., Lafferty, J., Rosenfeld, R., 2005. Semi-supervised learning with graphs. Ph.D. thesis. Carnegie Mellon University, language technologies institute, school of .
- Zhu, X., Suk, H.I., Wang, L., Lee, S.W., Shen, D., 2017. A novel relational regularization feature selection method for joint regression and classification in ad diagnosis. Medical Image Analysis 38, 205–214.